

Supporting online material for

Boron encapsulated in a liposome can be used for Combinational Neutron Capture Therapy

Jiyuan Li^{#1}, Qi Sun^{#2}, Chuanjie Lu¹, Han Xiao³, Zhibin Guo¹, Dongban Duan¹, Zizhu Zhang^{4,5}, Tong Liu⁵ and Zhibo Liu^{*1,2}

¹Beijing National Laboratory for Molecular Sciences, Radiochemistry and Radiation Chemistry Key Laboratory of Fundamental Science, College of Chemistry and Molecular Engineering, Peking University, Beijing 100871 (China)

²Peking University-Tsinghua University Center for Life Sciences, Beijing, 100871 (China)

³University of Chinese Academy of Sciences Beijing, 100049 (China)

⁴Beijing Nuclear Industry Hospital, Beijing, 100045 (China)

⁵Beijing Capture Tech Co., Ltd, Beijing, 102413 (China)

[#]The authors contributed equally to this paper.

^{*}To whom correspondence should be addressed. E-mail Z.L (zbliu@pku.edu.cn)

The file includes:

- 1) Supplementary Table 1 to 6
- 2) Supplementary Figure 1 to 11
- 3) NMR information (Description and Supplementary Figure 12-23)
- 4) HRMS information (Description and Supplementary Figure 24-27)

Supplementary tables and figures

Supplementary Table 1 No-Bonds parameter of MD simulations.

Type	C6	C12
H	0.0000E+00	0.0000E+00
HC	8.4640E-05	1.5129E-08
B	2.3406E-03	4.9373E-06
C	2.3406E-03	4.9373E-06
S	9.9840E-03	1.3075E-05

Supplementary Table 2 Bonds parameter of MD simulations.

Bonds	$b_0(\text{\AA})$	kb
H- B_α	1.19	2.6481e+07
H- B_β	1.19	2.6481e+07
H- B_γ	1.18	3.5909e+07
H- B_δ	1.18	3.5909e+07
H-C	1.09	1.2300e+07
S-C	1.67	3.0478e+06
C-C	1.63	8.5653e+05
C- B_α	1.63	8.7100e+06
C- B_β	1.63	4.7200e+06
B_α - B_β	1.78	1.0665e+06
B_α - B_γ	1.76	1.8519e+06
B_β - B_β	1.79	5.6200e+06
B_β - B_γ	1.78	2.6424e+06
B_β - B_δ	1.78	2.7200e+06
B_γ - B_δ	1.79	2.1847e+06
B_δ - B_δ	1.69	1.9257e+06

Supplementary Table 3 Angles parameter of MD simulations.

Angles	θ	Ka
S-C- B_α	114.00	1559.41
S-C- B_β	132.00	760.00
S-C-C	120.00	560.00
C- B_α -C	56.39	2100.95
C- B_α - B_β	124.00	730.00
HC-C- B_α	118.00	7474.41
HC-C- B_β	125.00	375.00
HC-C-C	120.00	505.00
H- B_α -C	120.00	390.00
H- B_α - B_β	132.22	390.00
H- B_β - B_α	119.00	2211.40
H- B_β - B_β	119.74	3398.91
H- B_β - B_γ	121.00	685.00
H- B_β - B_δ	132.00	760.00
H- B_γ - B_δ	121.00	685.00
H- B_γ - B_β	117.00	635.00
H- B_δ - B_γ	121.00	375.00
H- B_δ - B_δ	121.40	690.00
B_α -C- B_α	115.71	1201.92
B_α - B_β - B_β	97.40	469.00
B_α - B_β - B_γ	60.30	531.36
B_α - B_β - B_δ	103.00	420.00
B_β - B_α - B_β	106.75	503.00
B_β - B_β - B_γ	107.57	484.00
B_β - B_β - B_δ	59.90	508.93
B_β - B_γ - B_δ	60.30	531.36
B_β - B_δ - B_γ	59.90	508.93
B_γ - B_δ - B_δ	63.30	2254.27

Supplementary Table 4 Bilayer width and maximum density of BoPs by MD simulations.

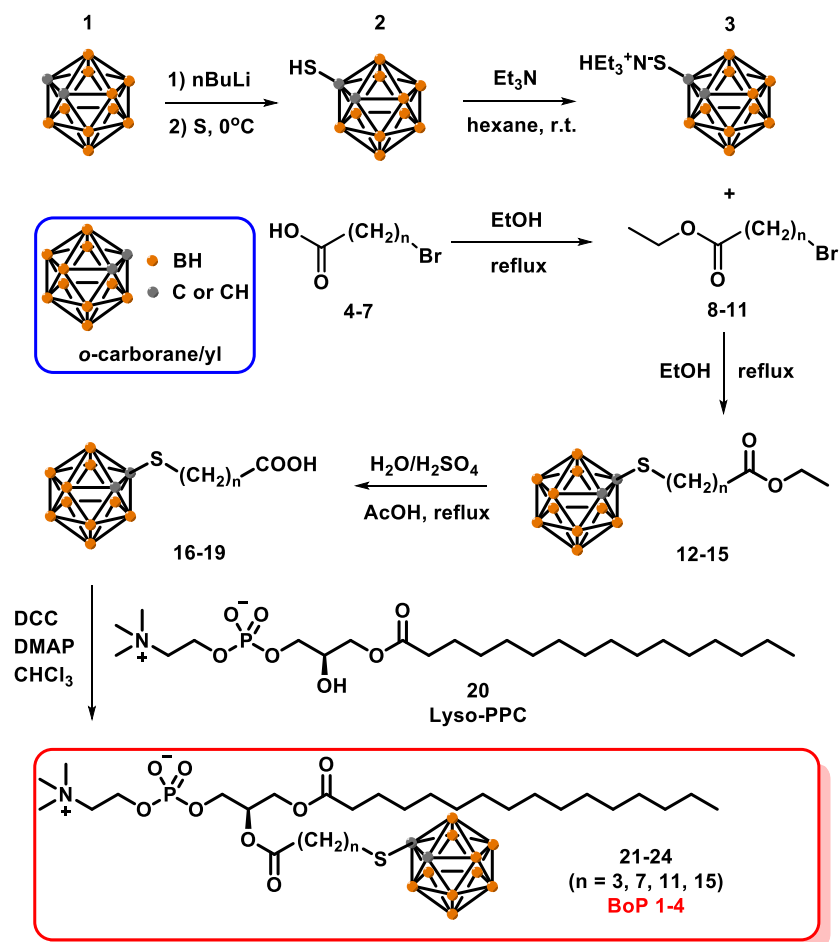
BoPs	Bilayer width (nm)	Maximum density (kg/m ³)
DPPC	4.83	1484.07
BoP-1	3.93	1509.98
BoP-2	4.65	1446.07
BoP-3	5.24	1382.70
BoP-4	5.60	1466.98

Supplementary Table 5 Biodistribution data and tumor-to-normal tissue ratio (T/N ratio) of boronsome in 4T1 bearing mice measured by ICP-OES 12 h post once injection of boronsome (500 mg/kg, i.v.). Data are means \pm SEM (n = 4 mice).

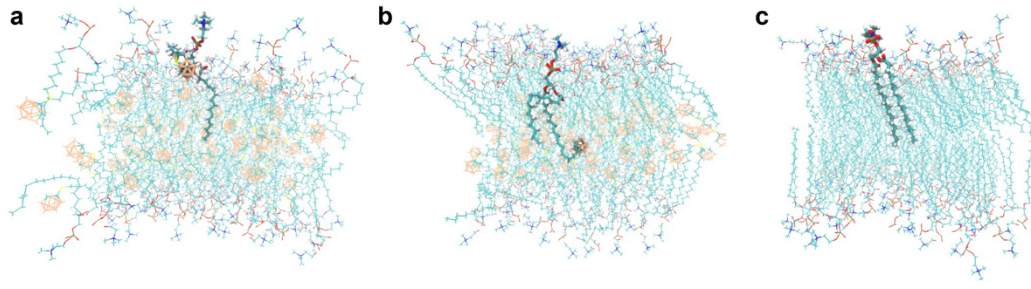
Tissues	Boron concentration (ppm)	T/N ratio
Tumor	93.25 \pm 2.7	-
Lung	1.50 \pm 0.1	63.59 \pm 2.3
Muscle	2.60 \pm 0.1	37.30 \pm 1.8
Brain	1.25 \pm 0.1	82.71 \pm 6.4
Fat	3.65 \pm 0.1	25.85 \pm 0.7
Bone	5.90 \pm 0.3	16.32 \pm 0.8
Heart	9.85 \pm 0.3	9.58 \pm 0.3
Blood	19.15 \pm 0.5	4.92 \pm 0.1
Liver	351.71 \pm 10.0	0.27 \pm 0.0
Spleen	205.45 \pm 8.0	0.47 \pm 0.0

Supplementary Table 6 Dose computations by Monte Carlo simulation using Simulation Environment for Radiotherapy Applications (SERA) system. The beam location is determined by the source geometry, the target point (X, Y, Z) represents the distance from the target to the source center. For dose estimation in BNCT, all of these dose components including B-10, gamma, N-14 and hydrogen need to be calculated.

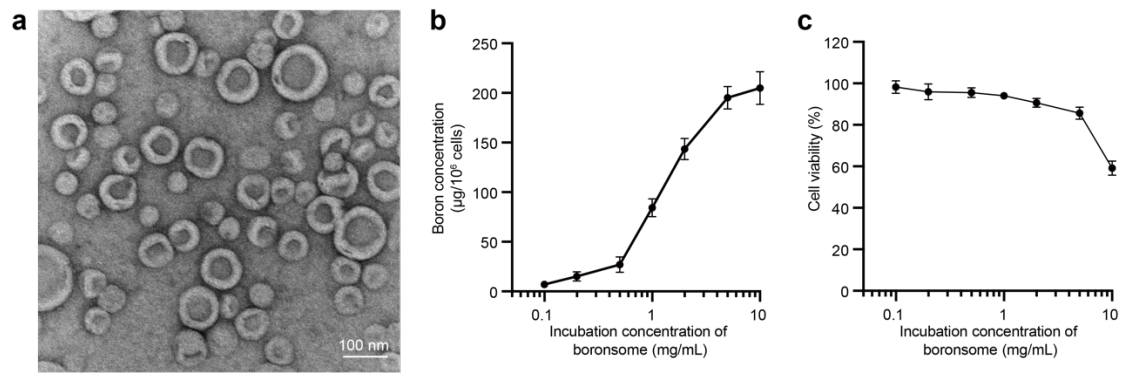
X (cm)	Y (cm)	Z (cm)	reg	Total dose rate (cGy/s)	B-10 dose rate (cGy/s)	Gamma dose rate (cGy/s)	N-14 dose rate (cGy/s)	Hydrogen dose rate (cGy/s)	Total dose (Gy)
0	-4.5	-0.00100	air	0.0372	0.0000	0.0167	0.0123	0.0082	0.6692
0	-4.5	-0.00135	tumor tissue	0.1014	0.0642	0.0167	0.0123	0.0082	1.8254
0	-4.5	-0.25140	tumor tissue	0.1141	0.0718	0.0189	0.0138	0.0097	2.0542
0	-4.5	-0.50120	normal tissue	0.0569	0.0128	0.0235	0.0099	0.0106	1.0236
0	-4.5	-0.75120	normal tissue	0.0547	0.0115	0.0236	0.0090	0.0106	0.9841
0	-4.5	-1.00100	normal tissue	0.0376	0.0061	0.0173	0.0048	0.0094	0.6769
0	-4.5	-1.25100	normal tissue	0.0337	0.0051	0.0153	0.0041	0.0093	0.6071
0	-4.5	-1.50100	normal tissue	0.0237	0.0030	0.0081	0.0024	0.0102	0.4271
0	-4.5	-1.70000	air	0.0194	0.0000	0.0068	0.0022	0.0103	0.3488
0	-4.5	-1.95000	air	0.0181	0.0000	0.0054	0.0021	0.0105	0.3256
0	-4.5	-2.00100	air	0.0175	0.0000	0.0038	0.0029	0.0107	0.3146



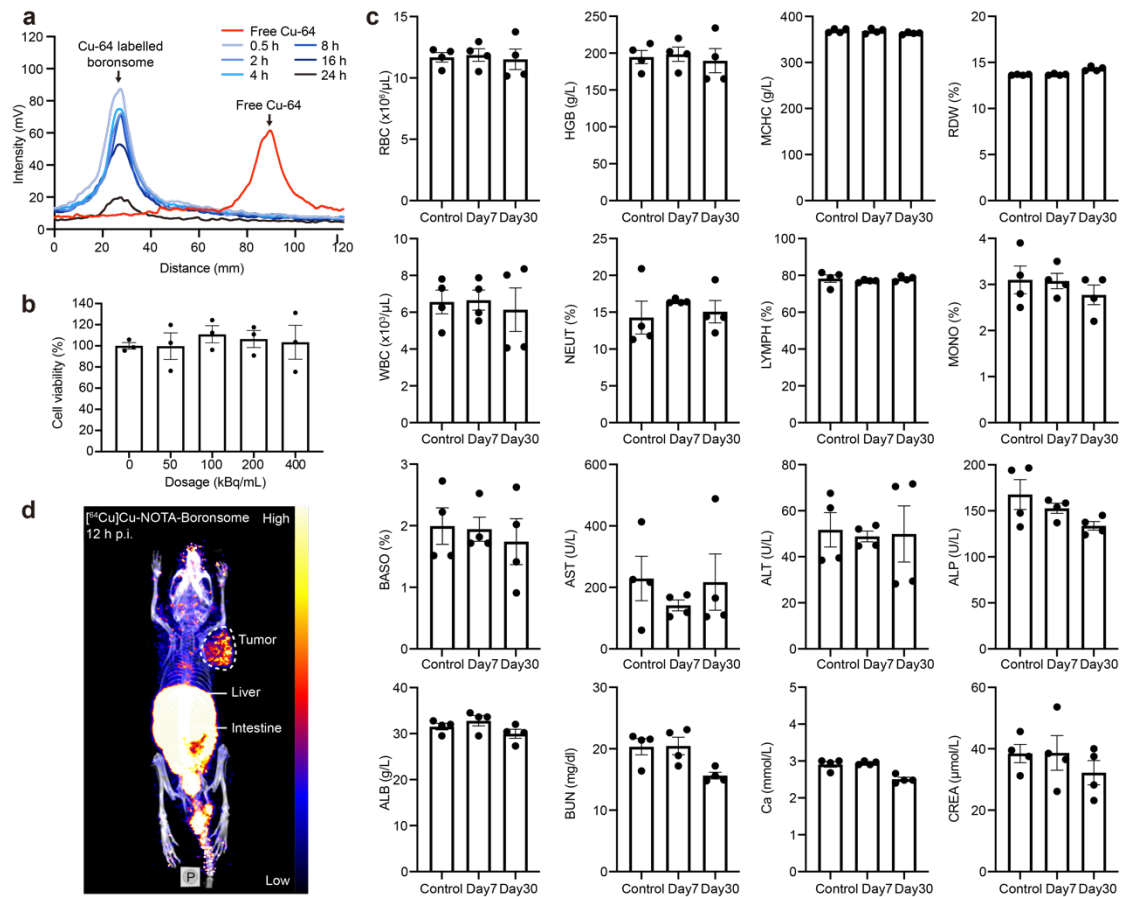
Supplementary Figure 1. Chemical synthesis of BoPs. Reagents and solvents were purchased from Sigma-Aldrich, Thermo Fisher or Novabiochem. All nuclear MR spectra were recorded at room temperature on a Bruker Avance 400 MHz or 500 MHz spectrometer. Signals are presented as ppm, and multiplicity identified as s = single, br = broad, d = doublet, t = triplet, q = quartet, m = multiplet; coupling constants in Hz. Concentration under reduced pressure was performed by rotary evaporation. Chemistry yields refer to isolated pure chemicals.



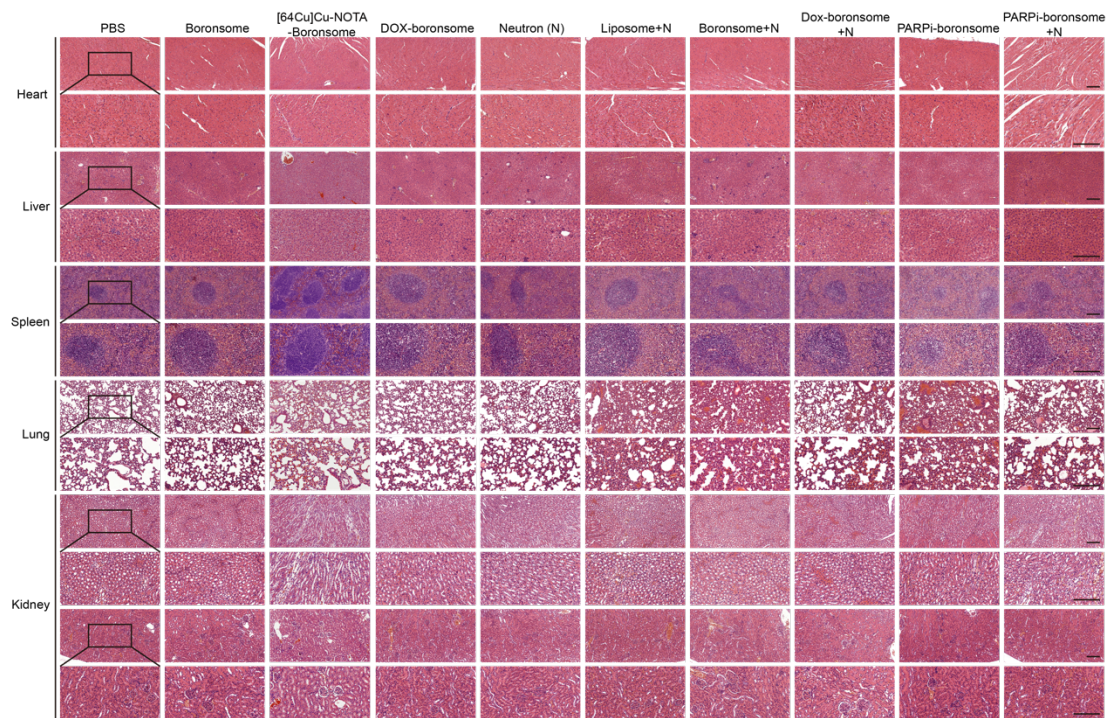
Supplementary Figure 2. Cross-section of liposomes by MD simulations. **a** BoP-2. **b** BoP-4. **c** DPPC.



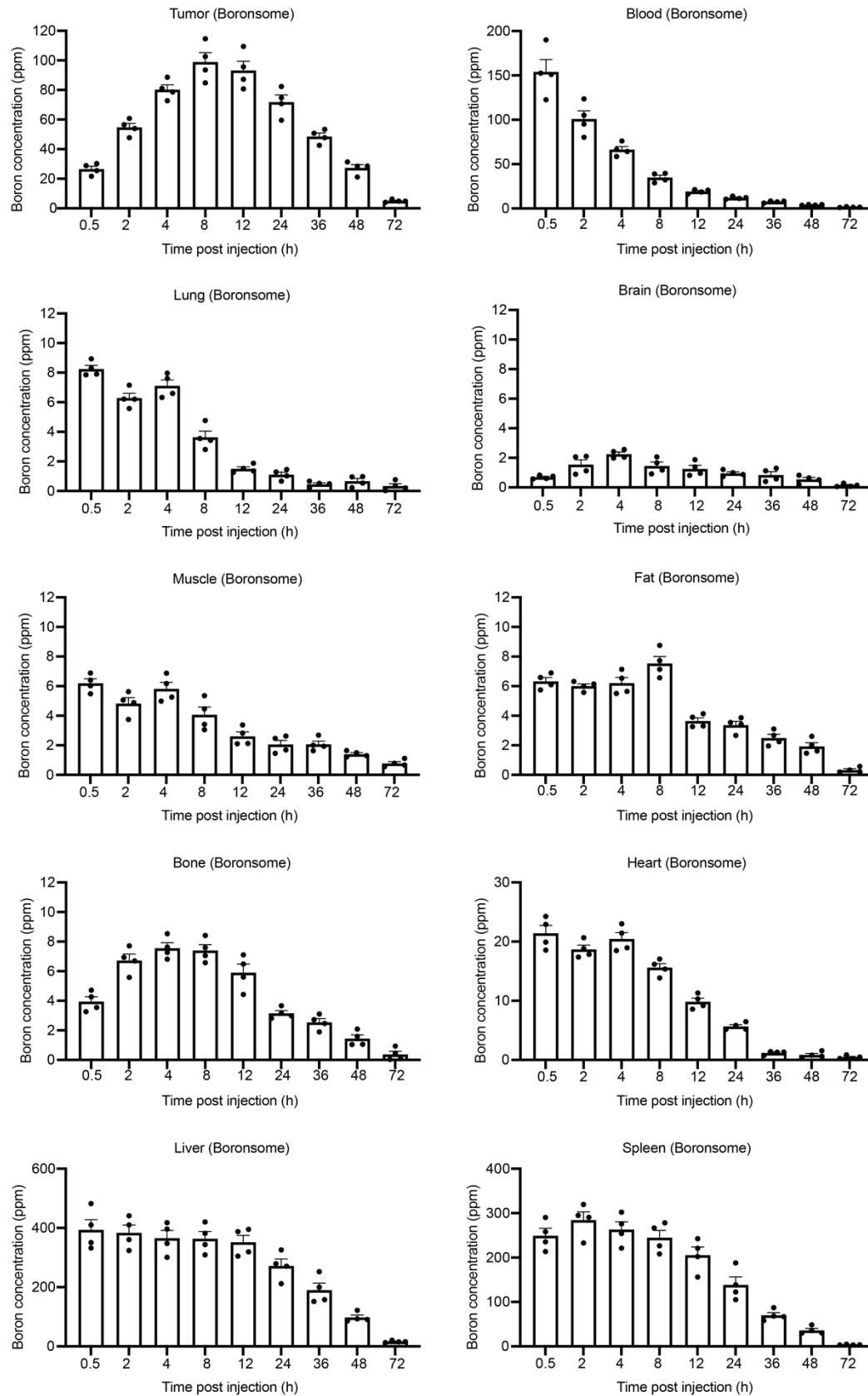
Supplementary Figure 3. Borosome presents uptake in line with clinical needs and exhibited good tolerance. **a** Imaging of borosomes by transmission electron microscopy (TEM). Three independent experiments were performed and representative results are shown. Scale bar, 100 nm. **b** Cellular boron uptake of 4T1 cells incubated with various concentrations of borosome for 24 h (n = 4). **c** Cell viability of 4T1 cells incubated with various concentrations of borosome for 24 h (n = 6). Data are means ± SEM. Source data are provided as a Source Data file.



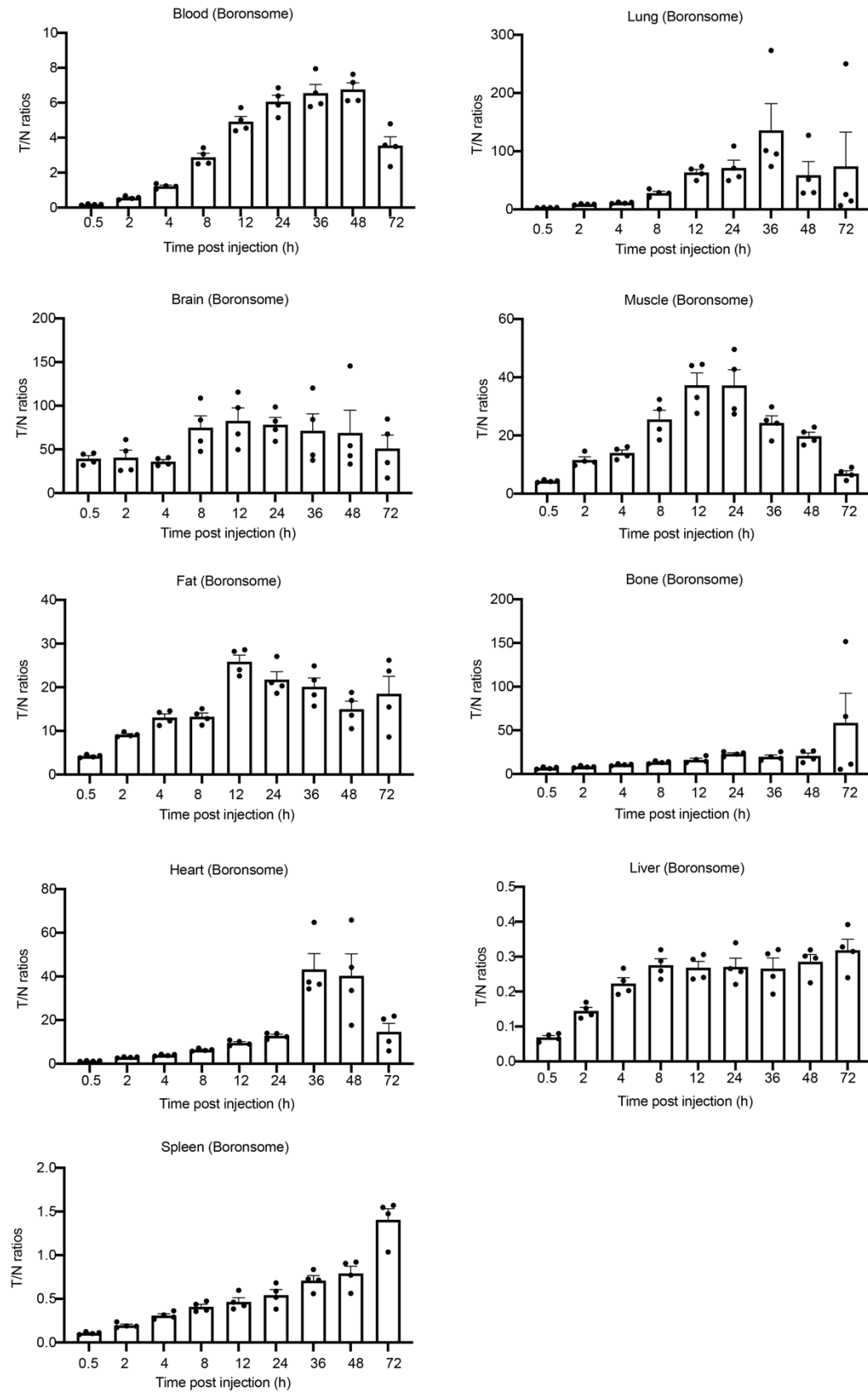
Supplementary Figure 4. Stability and biocompatibility of $[^{64}\text{Cu}]\text{Cu-NOTA-boronsomes}$. **a** Radio thin layer chromatography (radio-TLC) for the conformation of notable stability of $[^{64}\text{Cu}]\text{Cu-NOTA-boronsomes}$. **b** Survival fraction (n = 3) of 4T1 cells under various dosages of $[^{64}\text{Cu}]\text{Cu-NOTA-boronsome}$ after 24 h assessed with a CCK-8 assay. We picked a dosage (40 kBq, 2×10^4 cells) that far exceeds 1000-fold the activity of tumour region (200 kBq, about 10^8 cells), and exceed (300-fold) the activity of liver region (2000 kBq, about 3×10^8 cells), which has a highest uptake of $[^{64}\text{Cu}]\text{Cu-NOTA-boronsome}$ according to the PET study. **c** The blood routine and biochemical test of 4T1 tumor-bearing mice intravenously injected with $[^{64}\text{Cu}]\text{Cu-NOTA-boronsome}$ at day 7 and day 30 (n = 4). **d** Whole-body maximum intensity projection PET images of a 4T1 bearing mouse, 12 h after intravenous injection with $[^{64}\text{Cu}]\text{Cu-NOTA-boronsome}$. Tumors were circled with white dashed line. Data are means \pm SEM. Source data are provided as a Source Data file.



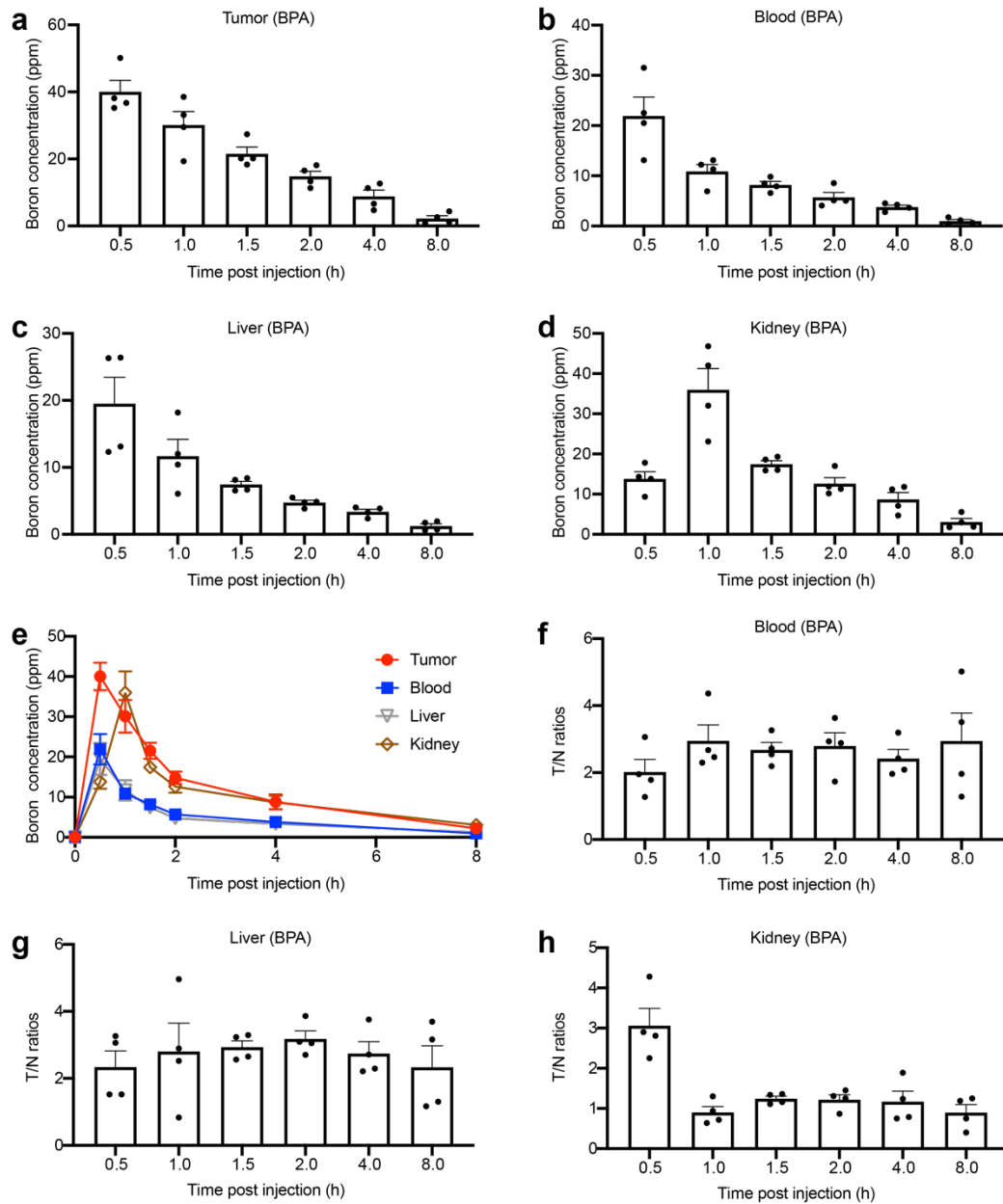
Supplementary Figure 5. Hematoxylin and eosin (H&E) staining of hearts, livers, spleens, lungs and kidneys obtained from 4T1 tumor bearing mice. Three independent experiments were performed and representative results are shown. Scale bar, 200 μ m.



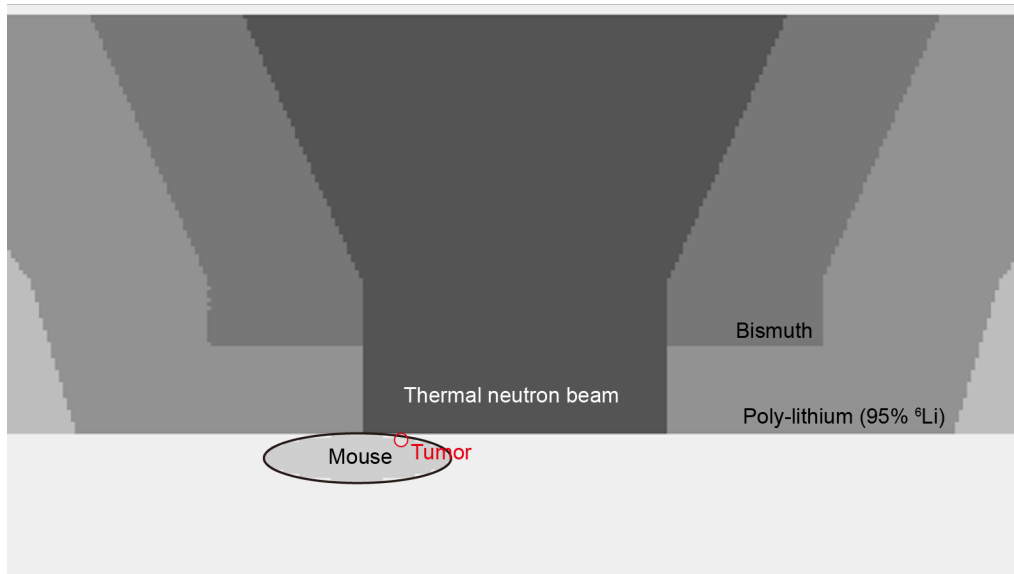
Supplementary Figure 6. Time-dependent boron concentration in tumor, blood, lung, brain, muscle, fat, bone, heart, liver, and spleen post once injection of boronsome (500 mg/kg, i.v.). Data are means \pm SEM ($n = 4$ mice). Source data are provided as a Source Data file.



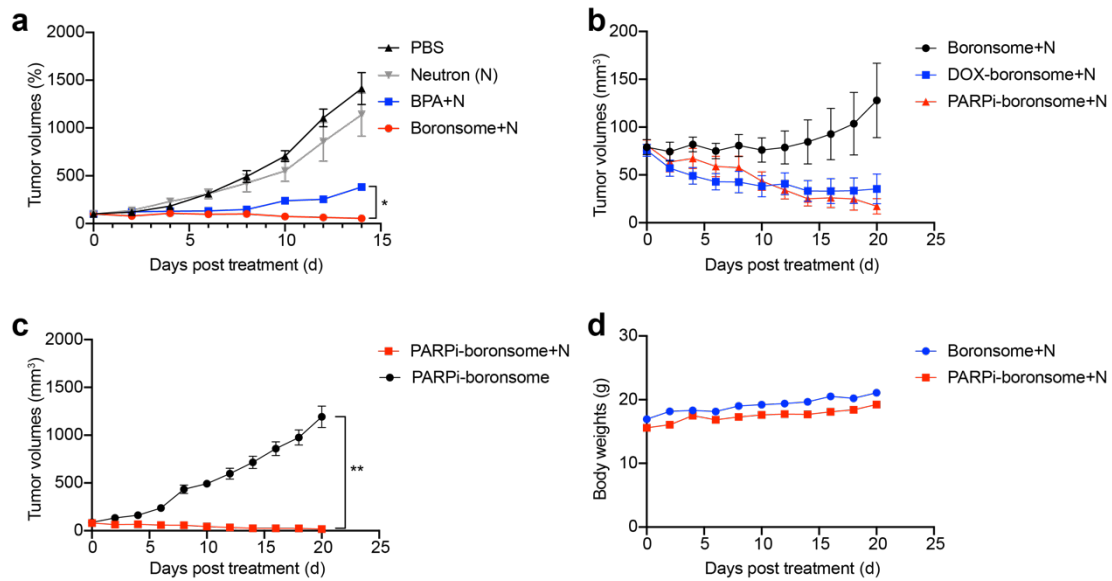
Supplementary Figure 7. Tumor-to-normal tissue ratio (T/N ratio) of blood, lung, brain, muscle, fat, bone, heart, liver, and spleen post once injection of boronsome (500 mg/kg, i.v.). Data are means ± SEM (n = 4 mice). Source data are provided as a Source Data file.



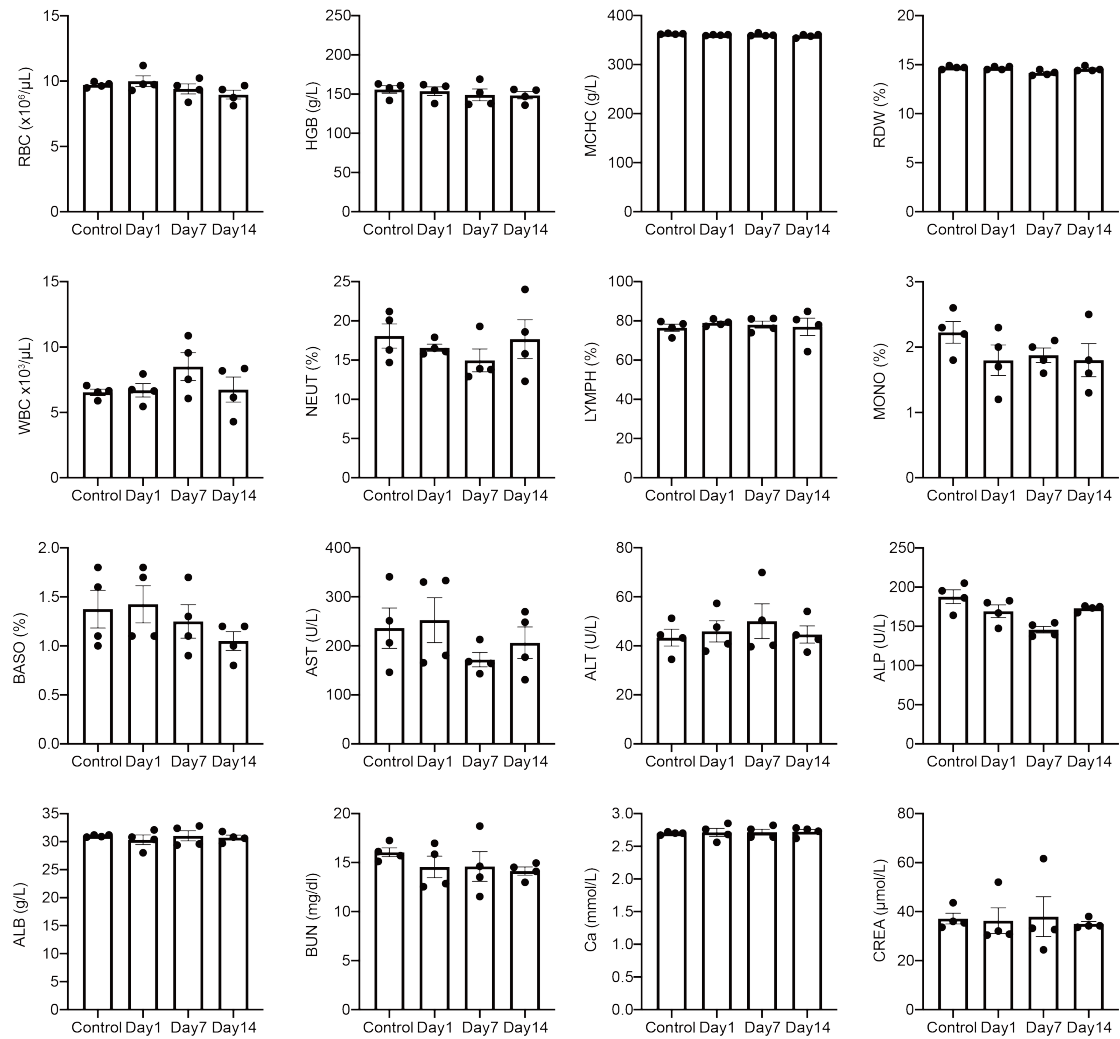
Supplementary Figure 8. Time-dependent boron concentration and T/N ratios of BPA in major organs. a-e Boron con in tumor, blood, liver, and kidney post once injection of BPA (500 mg/kg, i.v.). **f-h** Tumor-to-normal tissue ratio (T/N ratio) of blood, liver, and kidney post once injection of BPA (500 mg/kg, i.v.) Data are means ± SEM (n = 4 mice). Source data are provided as a Source Data file.



Supplementary Figure 9. SERA modeling.



Supplementary Figure 10. Changes of tumor volumes and weights over time in different groups of mice. **a** Average tumor increase fold ($n = 4$) of each group of mice treated with PBS, neutron (N), BPA+N, and boronsome+N. Paired t-test, $*p = 0.0366$. **b** Average tumor volumes ($n = 9$) of each group of mice treated with Boronsome+N, Dox-boronsome+N, and PARPi-boronsome+N. **c** Average tumor volumes ($n = 9$) of each group of mice treated with PARPi-boronsome and PARPi-boronsome+N. Paired t-test, $**p = 0.0019$. **d** Average body weights ($n = 9$) of each group of mice treated with boronsome+N or PARPi-boronsome+N. Data are means \pm SEM. Source data are provided as a Source Data file.



Supplementary Figure 11. The blood routine and biochemical test of 4T1 tumor-bearing mice intravenously injected with 500 mg/kg boronsome at day 1, day 7 and day 14 ($n = 4$). Data are means \pm SEM. Source data are provided as a Source Data file.

NMR information

Compound 12

¹H NMR (400 MHz, chloroform-d): δ 4.16 (m, 2H), 3.75 (s, 1H), 2.97 (t, 2H), 2.39 (t, 2H), 1.91 (p, 2H), 1.27 (t, 3H), 0.80-3.40 (br, 10H) (85 % yield).

Compound 13

¹H NMR (400 MHz, chloroform-d): δ 4.13 (q, 2H), 3.73 (s, 1H), 2.90 (t, 2H), 2.29 (t, 2H), 1.49 (m, 10H), 1.26 (t, 3H), 0.80-3.40 (br, 10H) (86 % yield).

Compound 14

¹H NMR (400 MHz, chloroform-d): δ 4.12 (q, 2H), 3.72 (s, 1H), 2.90 (t, 2H), 2.28 (t, 2H), 1.57 (tt, 4H), 1.26 (m, 17H), 0.80-3.40 (br, 10H) (89 % yield).

Compound 15

¹H NMR (400 MHz, chloroform-d): δ 4.12 (q, 2H), 3.72 (s, 1H), 2.90 (t, 2H), 2.28 (t, 2H), 1.58 (m, 4H), 1.26 (m, 25H), 0.80-3.40 (br, 10H) (82 % yield).

Compound 16

¹H NMR (400 MHz, chloroform-d): δ 3.74 (s, 1H), 2.99 (t, 2H), 2.48 (t, 2H), 1.93 (p, 2H), 0.80-3.40 (br, 10H) (78 % yield).

Compound 17

¹H NMR (400 MHz, chloroform-d): δ 3.72 (s, 1H), 2.90 (t, 2H), 2.36 (t, 2H), 1.60 (dp, 4H), 1.34 (m, 6H), 0.80-3.40 (br, 10H) (79 % yield).

Compound 18

¹H NMR (400 MHz, chloroform-d): δ 3.72 (q, 1H), 2.90 (t, 2H), 2.35 (t, 2H), 1.59 (dp, 4H), 1.28 (m, 14H), 0.80-3.40 (br, 10H) (83 % yield).

Compound 19

¹H NMR (400 MHz, chloroform-d): δ 3.72 (s, 1H), 2.90 (t, 2H), 2.35 (t, 2H), 1.59 (dp, 4H), 1.25 (s, 22H), 0.80-3.40 (br, 10H) (75 % yield).

Compound 21

¹H NMR (400 MHz, chloroform-d): δ 0.80-3.40 (br, 10H), 0.88 (m, 3H), 1.26 (s, 24H), 1.58 (d, 2H), 1.91 (p, 2H), 2.31 (p, 2H), 2.44 (t, 2H), 2.98 (t, 2H), 3.33 (s, 9H), 3.77 (s, 1H), 4.02 (m, 7H), 4.44 (s, 2H) (38 % yield). C₃₀H₆₆B₁₀NO₈PS, m/z found 740.52.

Compound 22

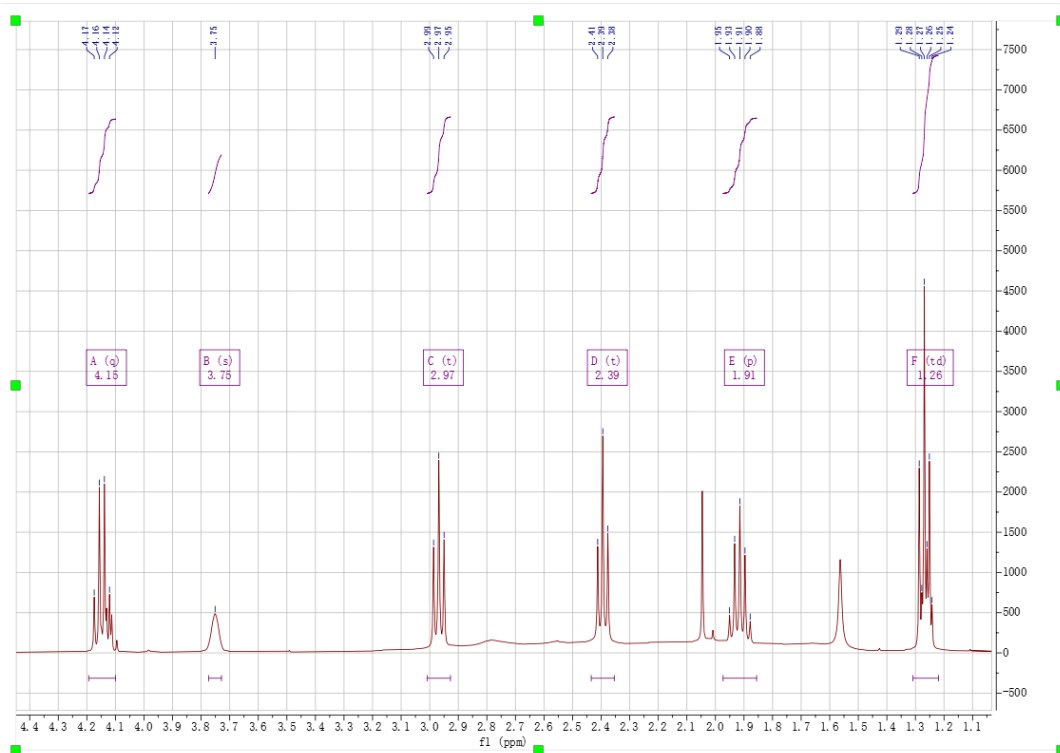
¹H NMR (400 MHz, chloroform-d): δ 0.80-3.40 (br, 10H), 0.88 (t, 3H), 1.29 (d, 30H), 1.58 (dq, 6H), 2.33 (t, 4H), 2.90 (t, 2H), 3.34 (t, 9H), 3.73 (s, 1H), 3.79 (m, 5H), 4.09 (d, 2H), 4.41 (s, 2H) (33 % yield). C₃₄H₇₄B₁₀NO₈PS, m/z found 796.72.

Compound 23

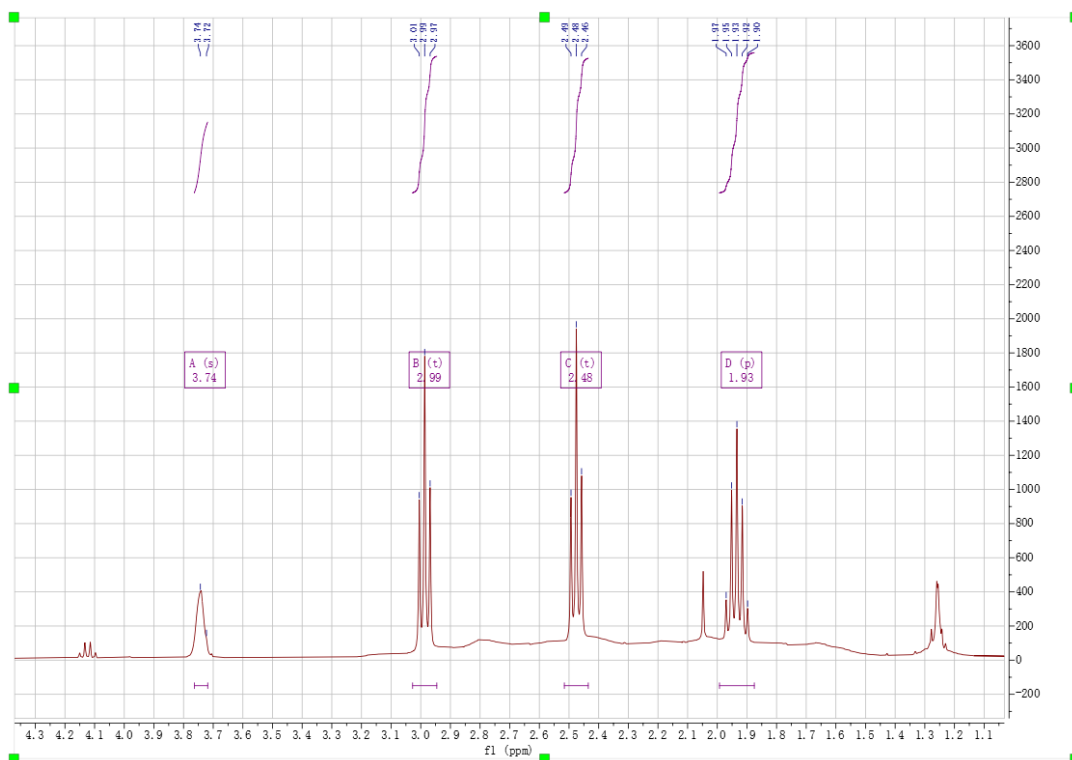
¹H NMR (400 MHz, chloroform-d): δ 0.80-3.40 (br, 10H), 0.87 (t, 3H), 1.29 (d, 38H), 1.58 (m, 6H), 2.33 (t, 4H), 2.90 (t, 2H), 3.34 (t, 9H), 3.73 (s, 1H), 3.85 (m, 5H), 4.08 (dd, 2H), 4.41 (s, 2H) (36 % yield). C₃₈H₈₂B₁₀NO₈PS, m/z found 852.69.

Compound 24

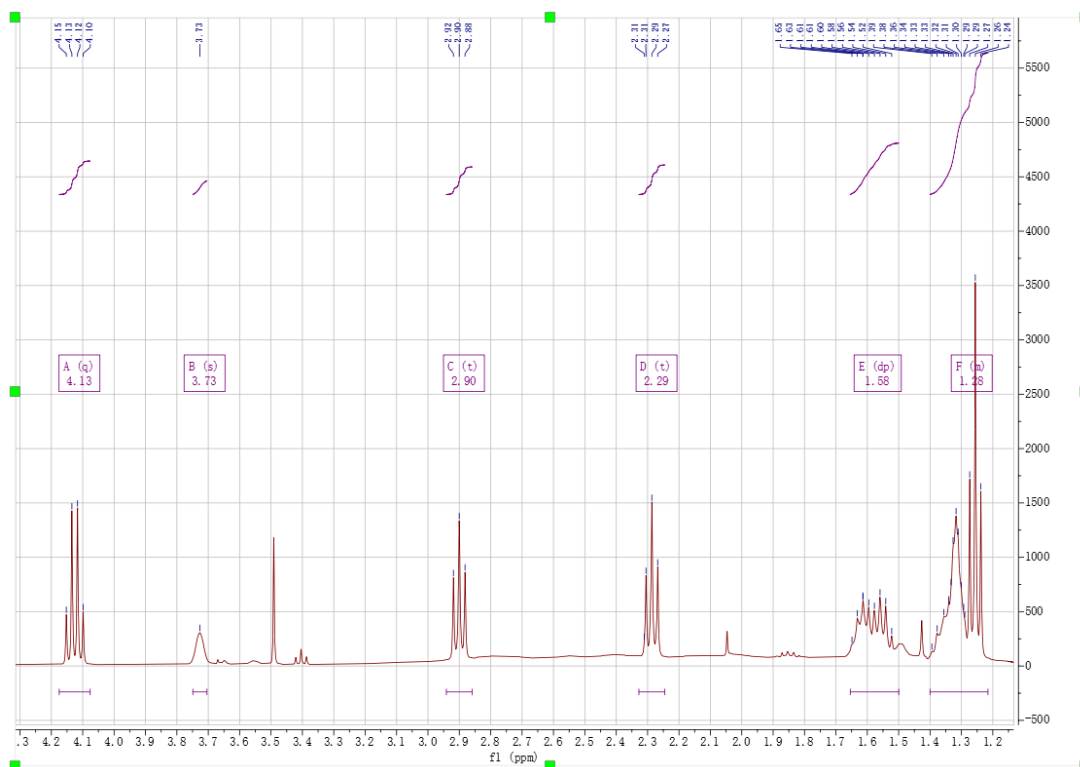
¹H NMR (400 MHz, chloroform-d): δ 0.80-3.40 (br, 10H), 0.87 (m, 3H), 1.25 (d, 46H), 1.58 (m, 6H), 2.33 (t, 4H), 2.90 (t, 2H), 3.31 (t, 9H), 3.72 (s, 1H), 3.88 (d, 5H), 4.08 (d, 2H), 4.36 (s, 2H) (22 % yield). C₄₂H₉₀B₁₀NO₈PS, m/z found 908.43.



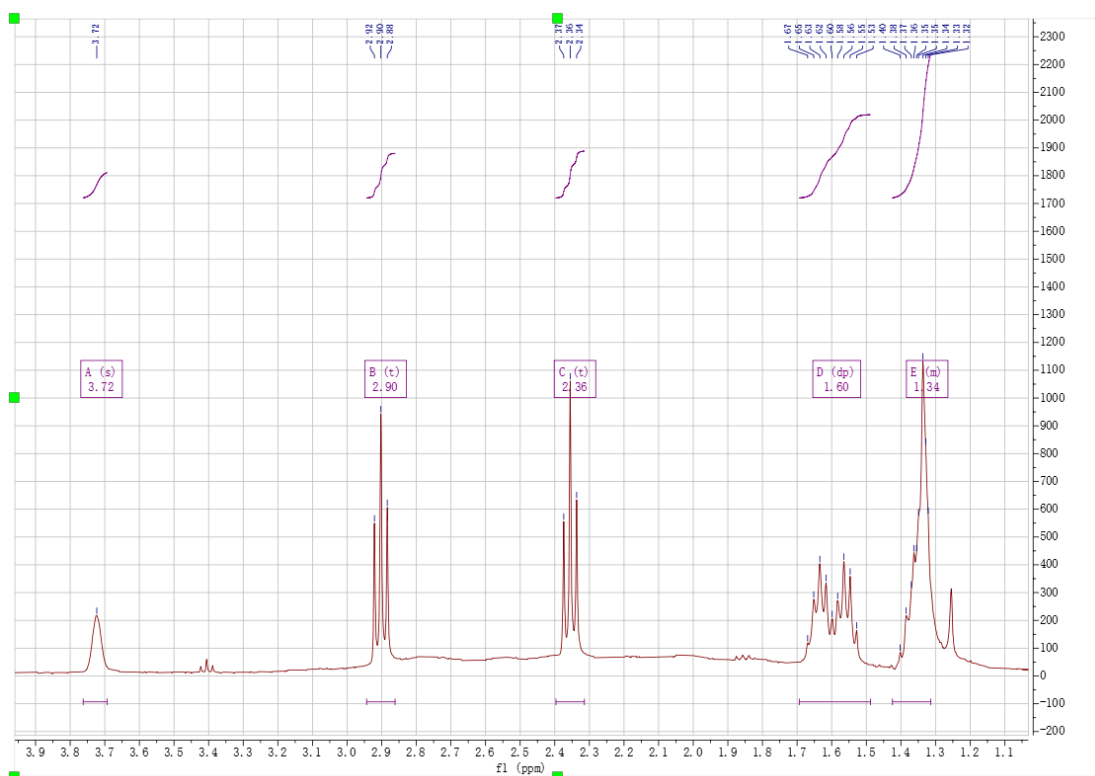
Supplementary Figure 12. $^1\text{H-NMR}$ spectrum of compound 12.



Supplementary Figure 13. $^1\text{H-NMR}$ spectrum of compound 13.



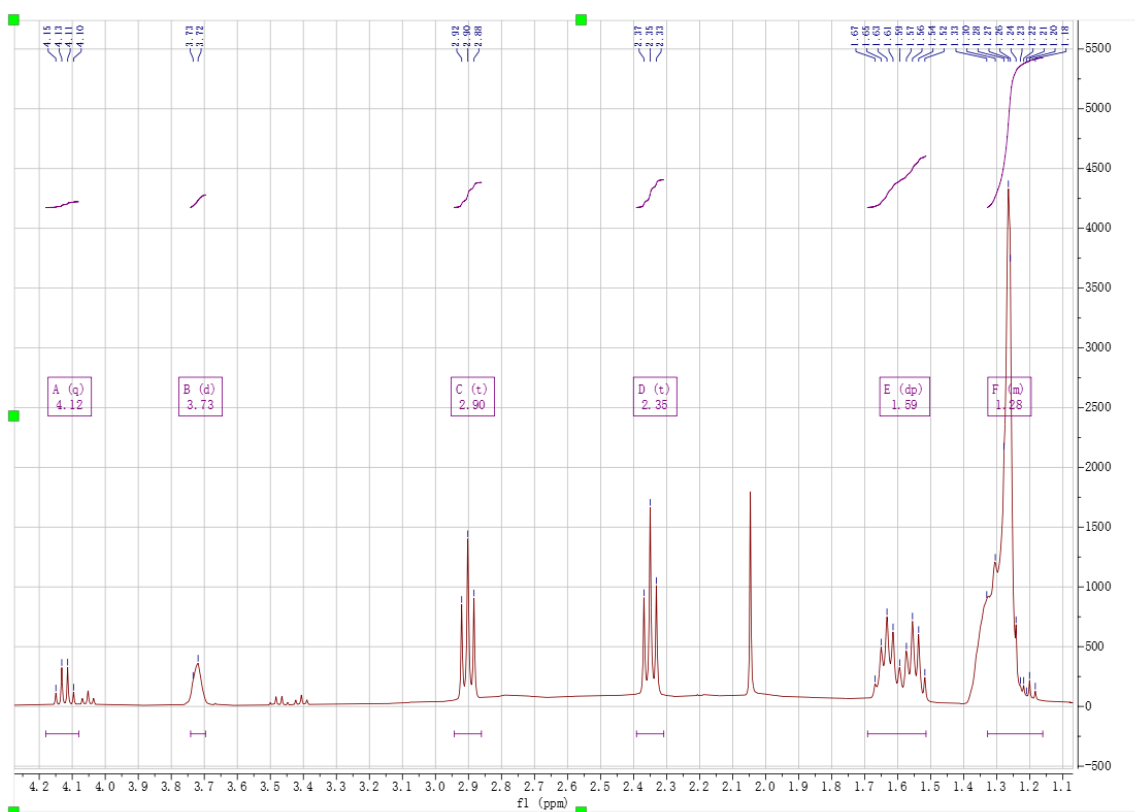
Supplementary Figure 14. $^1\text{H-NMR}$ spectrum of compound 14.



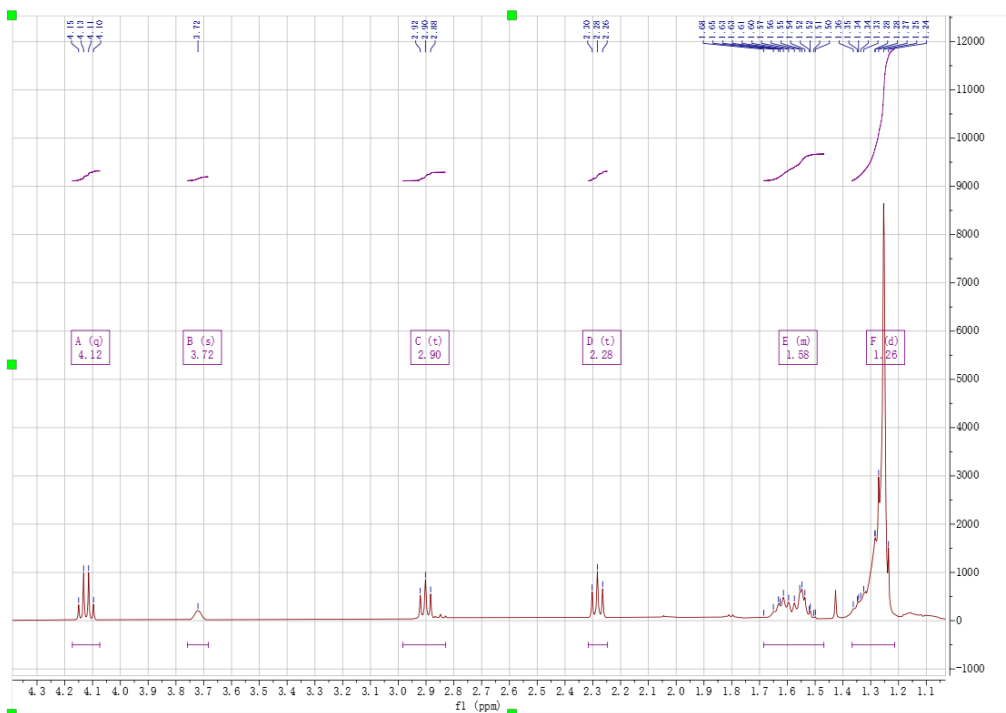
Supplementary Figure 15. $^1\text{H-NMR}$ spectrum of compound 15.



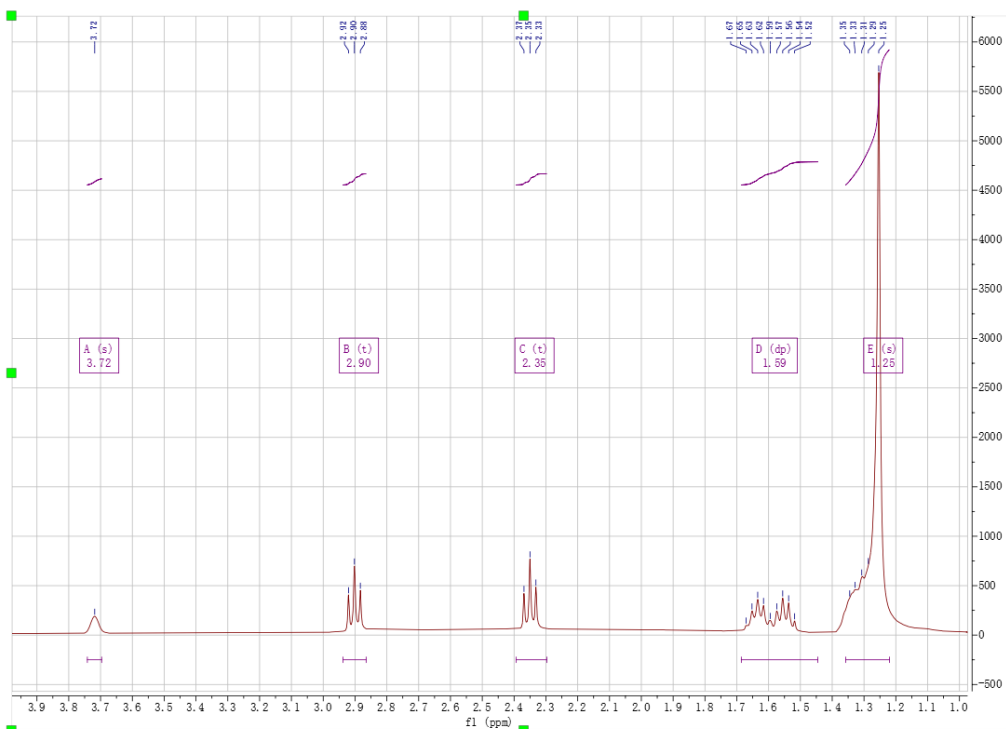
Supplementary Figure 16. $^1\text{H-NMR}$ spectrum of compound 16.



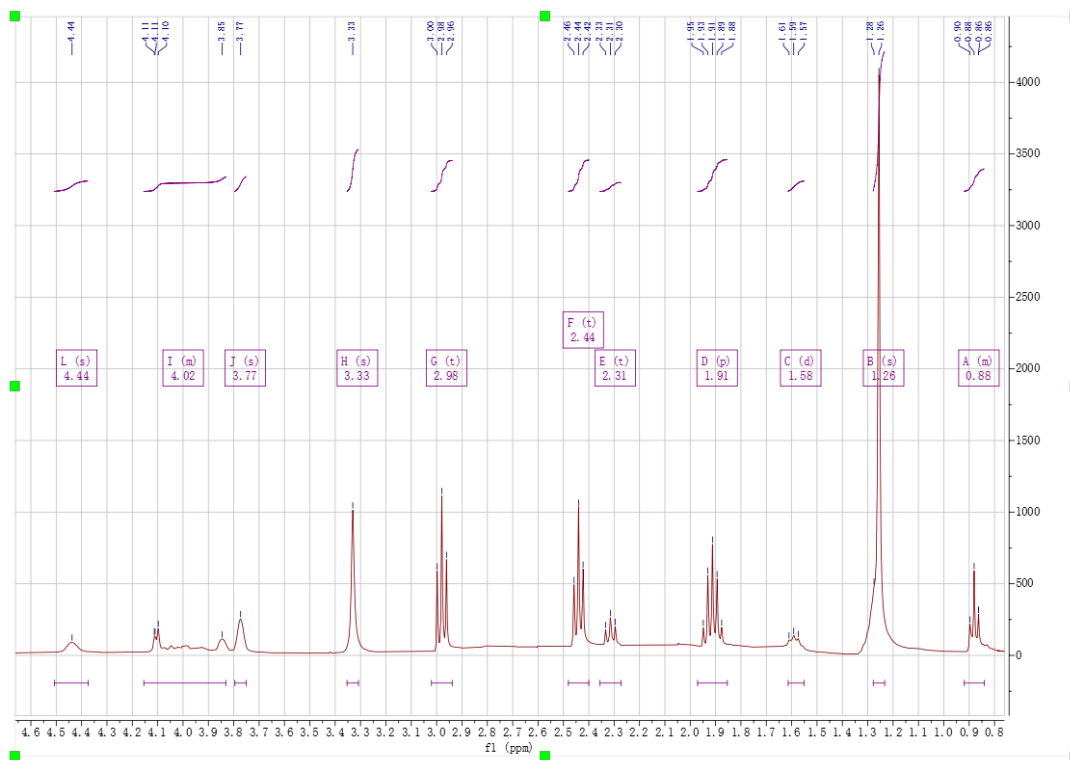
Supplementary Figure 17. $^1\text{H-NMR}$ spectrum of compound 17.



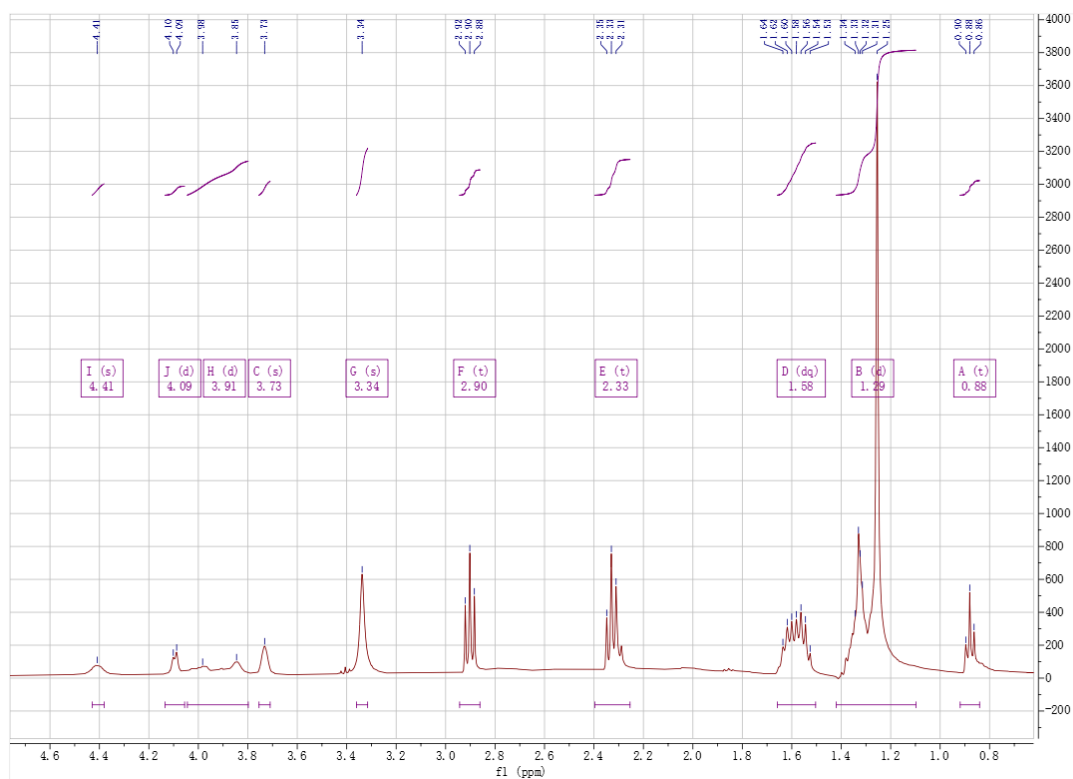
Supplementary Figure 18. ¹H-NMR spectrum of compound 18.



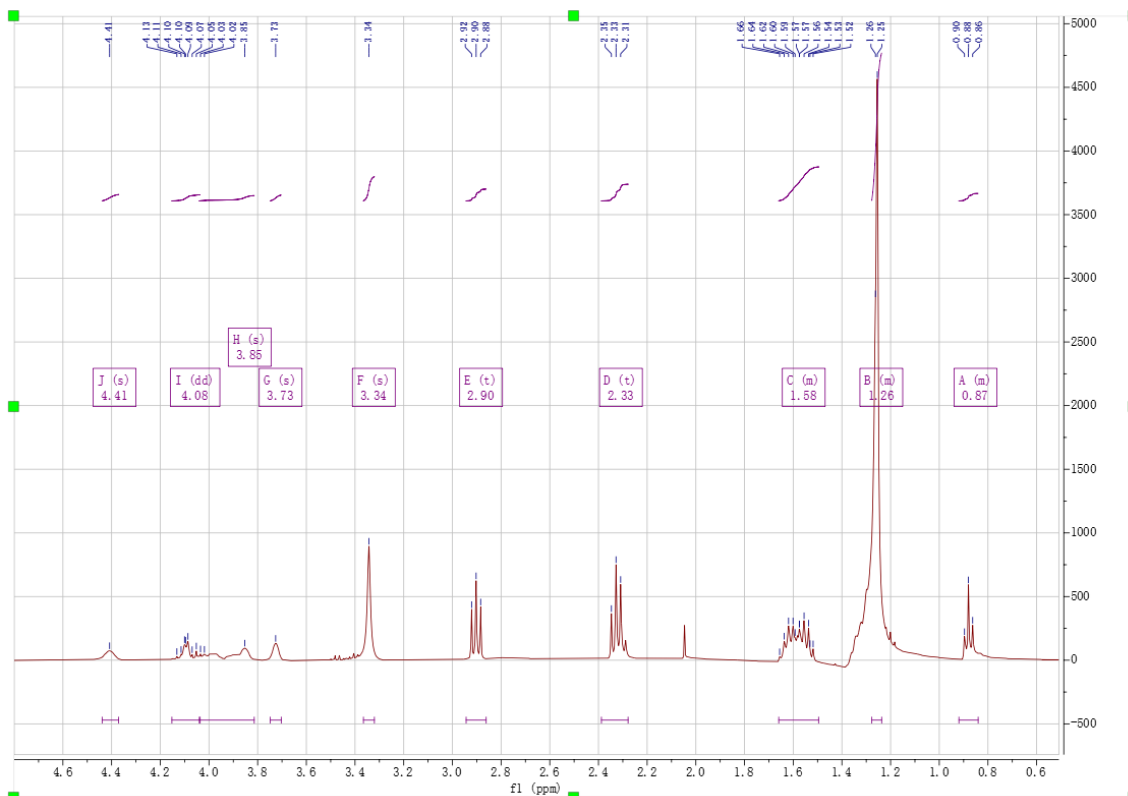
Supplementary Figure 19. ¹H-NMR spectrum of compound 19.



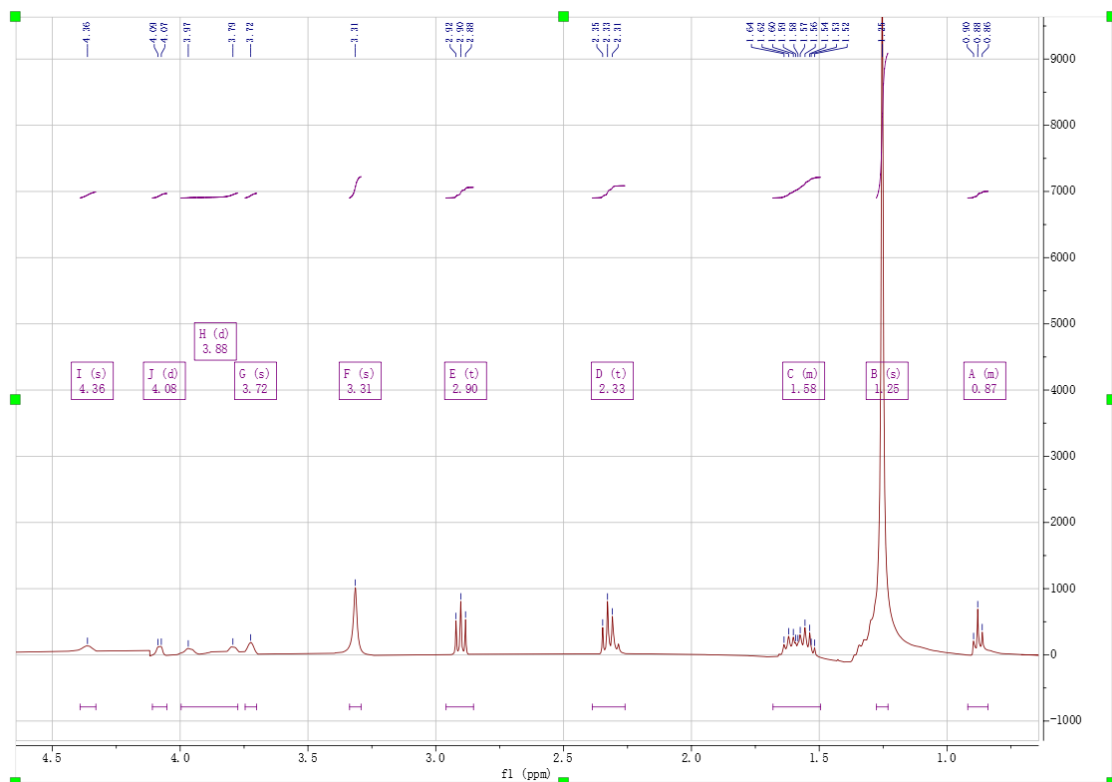
Supplementary Figure 20. $^1\text{H-NMR}$ spectrum of compound 21.



Supplementary Figure 21. $^1\text{H-NMR}$ spectrum of compound 22.



Supplementary Figure 22. $^1\text{H-NMR}$ spectrum of compound 23.



Supplementary Figure 23. $^1\text{H-NMR}$ spectrum of compound 24.

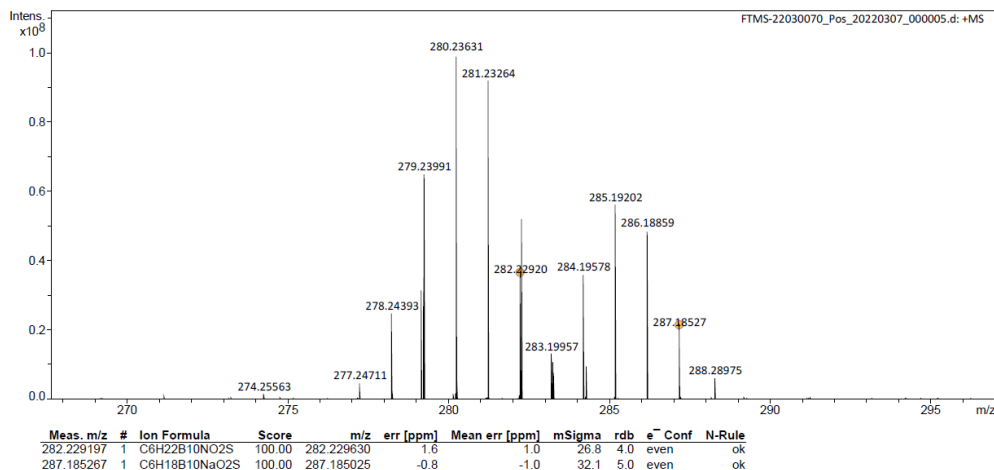
HRMS information

Peking University Mass Spectrometry Sample Analysis Report

Analysis Info

Analysis Name FTMS-22030070_Pos_20220307_000005.d
Sample 4C-COOH
Comment

Acquisition Date 3/7/2022 10:32:16 AM
Instrument Bruker Solarix XR FTMS
Operator Peking University



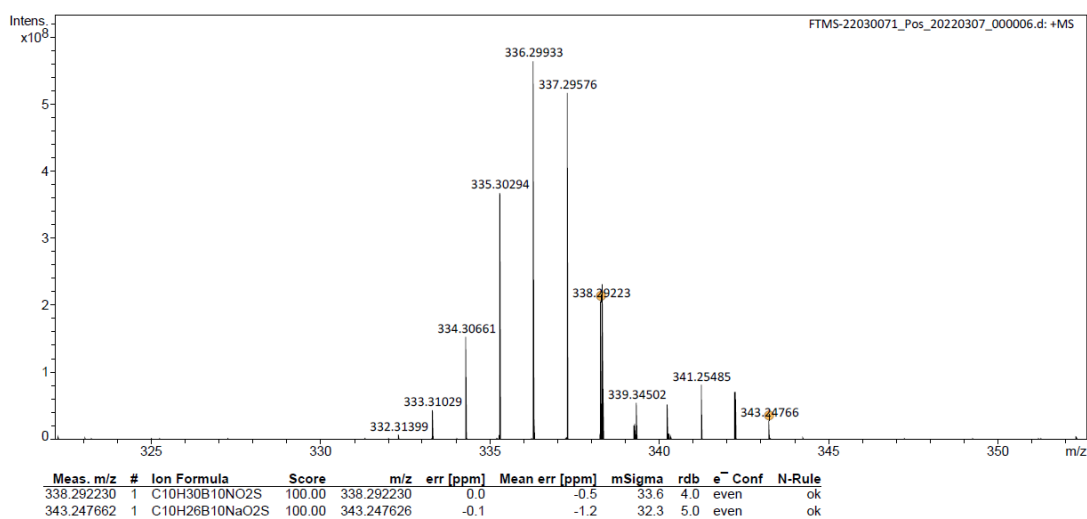
Supplementary Figure 24. High-resolution mass spectrum of compound 16.

Peking University Mass Spectrometry Sample Analysis Report

Analysis Info

Analysis Name FTMS-22030071_Pos_20220307_000006.d
Sample 8C-COOH
Comment

Acquisition Date 3/7/2022 10:23:38 AM
Instrument Bruker Solarix XR FTMS
Operator Peking University



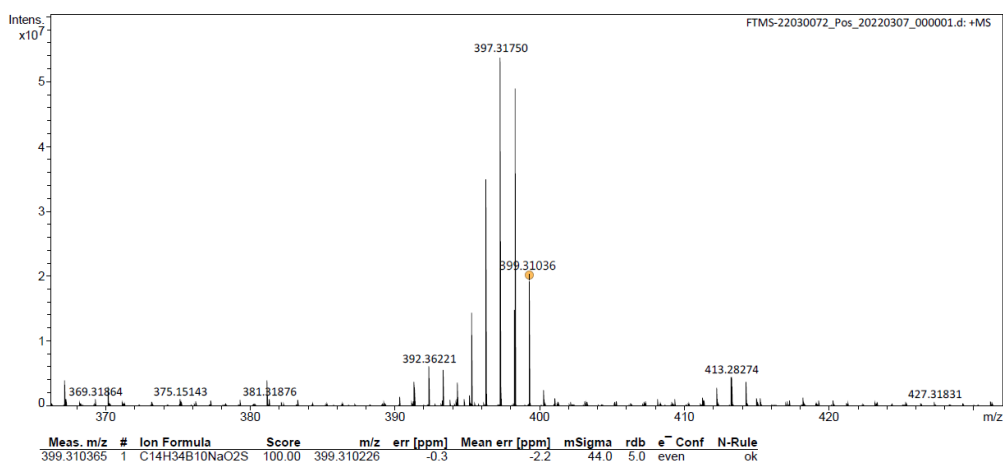
Supplementary Figure 25. High-resolution mass spectrum of compound 17.

Peking University Mass Spectrometry Sample Analysis Report

Analysis Info

Analysis Name FTMS-22030072_Pos_20220307_000001.d
Sample 12CCOOH
Comment

Acquisition Date 3/7/2022 10:12:34 AM
Instrument Bruker Solarix XR FTMS
Operator Peking University



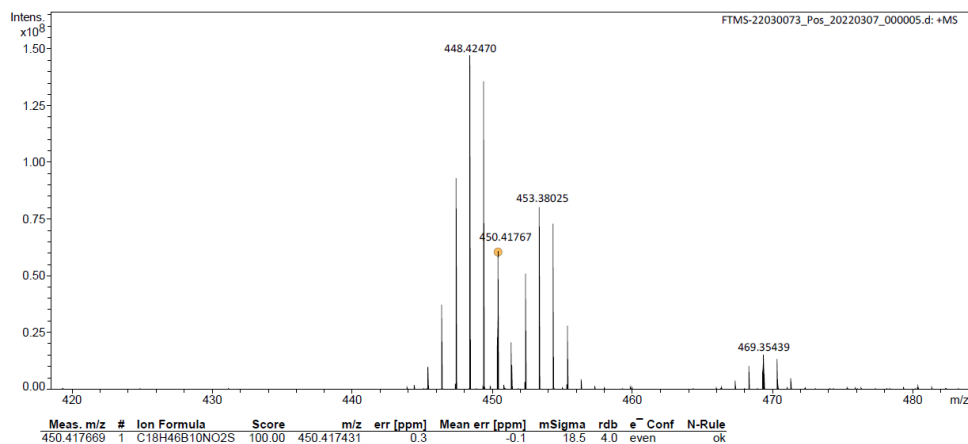
Supplementary Figure 26. High-resolution mass spectrum of compound 18.

Peking University Mass Spectrometry Sample Analysis Report

Analysis Info

Analysis Name FTMS-22030073_Pos_20220307_000005.d
Sample 16C-COOH
Comment

Acquisition Date 3/7/2022 10:07:10 AM
Instrument Bruker Solarix XR FTMS
Operator Peking University



Supplementary Figure 27. High-resolution mass spectrum of compound 19.